Paper Number: **425**

Analysis and Sizing of Composite Anisogrid Cylindrical Structures without Skin

James Ainsworth

Ainsworth J. James, Collier Research, Corp., 760 Pilot House Dr., Newport News, VA U.S.A.
Niemann Steffan, DLR, Lilienthalplatz 7 38108 Braunschweig, Germany.

ABSTRACT

The focus of this work is sizing of cylindrical structures, using composite anisogrid structural concepts and evaluating the efficiency of the grid concept with and without skin. The anisogrid structural concept was developed for wooden and metal airplanes more than 60 years ago. Currently, anisogrid composite structures are being evaluated for modern aircraft and space launch structures. Examples of the anisogrid structural concept are shown in Figure 1.

This paper will describe the analytical sizing approach and failure analysis methods for cylindrical anisogrid structure with and without skin. The anisogrid concepts without skin exhibit different failure methods than a grid structure where the ribs are supported longitudinally on one edge by the skin. Automated analysis methods were implemented in the commercial sizing software HyperSizer to calculate the critical strength and buckling margin of safety of the grid stiffener ribs without skin. The analytical methods are verified against other published analytical models and with detailed linear and non-linear finite element models. The panel level ABD stiffness and local strain is verified with NASTRAN finite element models of anisogrid panels without skin. After verifying the panel-level stiffness and local strain response, the analytically-computed global buckling Eigenvalue, computed using Rayleigh-Ritz SS8, is verified against a published analytical method and a linear, FEA numerical eigenvalue solution.

Ainsworth J. James, Collier Research, Corp., 760 Pilot House Dr., Newport News, VA U.S.A.
Niemann Steffan, DLR, Lilienthalplatz 7 38108 Braunschweig, Germany.

INTRODUCTION

The anisogrid structural concept was developed for wooden and metal airplanes more than 60 years ago. Currently, anisogrid composite structures are being evaluated for modern aircraft and space launch structures. Some examples of this anisogrid structural concept are depicted in Figure 1.

This work focuses on sizing a cylindrical structure using different configurations of grid stiffened concepts, with and without skin. For the grid concept without skin, the load is carried by rectangular members arranged in a circumferential, helical and axial truss structure.

Three structural concepts are sized using the commercial structural sizing software, HyperSizer. HyperSizer is an automated sizing tool that is valuable for sizing the anisogrid structure. Using the smeared sizing approach, the software has the ability to vary the rib spacing, height, angle and thickness variables without modifying a FE mesh. This document summarizes the HyperSizer sizing results and analytical methods for anisogrid panel concepts, with and without skin. The analytical methods used are verified with published analytical methods [1] and with detailed FEA verification models.

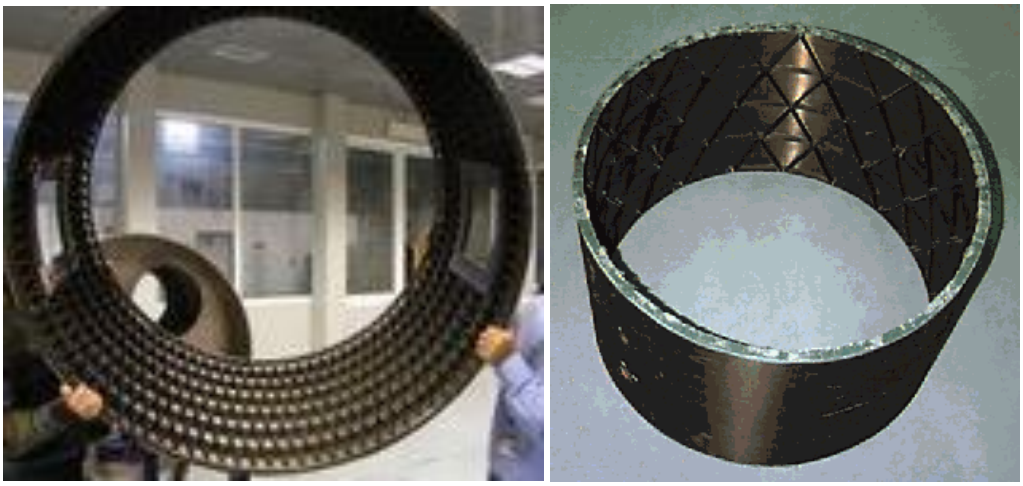

Figure 1. Examples of Anisogrid Structure

Ainsworth J. James, Collier Research, Corp., 760 Pilot House Dr., Newport News, VA U.S.A.
Niemann Steffan, DLR, Lilienthalplatz 7 38108 Braunschweig, Germany.

Structural Concept 1 Anisogrid with circumferential & helical ribs, no skin	Structural Concept 2 Anisogrid with circumferential, helical and axial ribs, no skin	Structural Concept 3 Anisogrid with circumferential & helical ribs, with skin
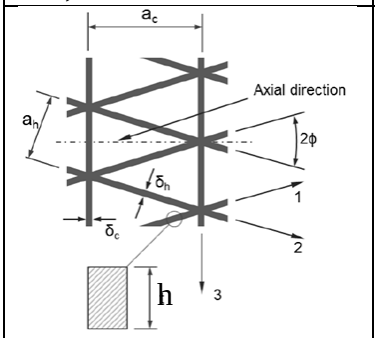	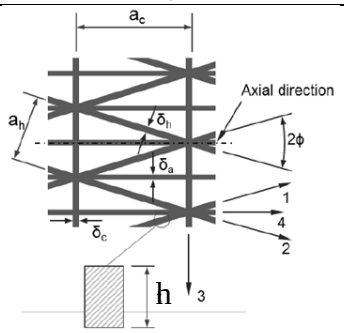	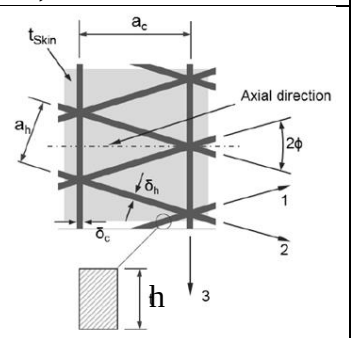

Figure 2. Anisogrid Structural concepts

Figure 2 illustrates the anisogrid structural concepts that were evaluated. For all anisogrid structural concepts the angle between circumferential and helical ribs is variable. For structural concept 1, the load carrying elements are arranged in circumferential and helical directions so there are no axial ribs to provide stiffness in the primary loading direction. Additionally, there is no skin to provide stability to the stiffening ribs. For structural concept 2 axial ribs are included to provide stiffness in the primary load direction. As with the previous concepts, there is no skin to provide stability to the ribs. For structural concept 3 skin is included to support the circumferential and helical ribs and the skin is not permitted to buckle prior to ultimate load. For all structural concepts the angle ribs are the same thickness and height. A producibility constraint is the minimum allowable rib spacing 100 millimeters.

A prismatic cylindrical barrel section is considered for sizing the structural concepts. The barrel dimensions are listed in table 1.

TABLE I. STRUCTURAL DIMENSIONS

R (mm)	**L (mm)**
2000	6000

TABLE II. INTERNAL LOAD

Load Case	**Nx (N/mm)**	**Ny (N/mm)**	**Nxy (N/mm)**
1	-592	0	0
2	-592	0	65
3	-198	0	160

For each structural concept the ribs are analyzed with effective stiffness properties. The strength of the ribs is evaluated against an axial strain limit. The rib design properties are listed in table 3. For the anisogrid concept with skin, a AS4/3502 Gr/Ep tape is considered, design properties are listed in table 4.

Ainsworth J. James, Collier Research, Corp., 760 Pilot House Dr., Newport News, VA U.S.A.
Niemann Steffan, DLR, Lilienthalplatz 7 38108 Braunschweig, Germany.

TABLE III. MATERIAL PROPERTIES - UNIDIRECTIONAL RIBS

E_1 (GPa)	v12	**etu1** (μmm/mm)	**ecu1** (μmm/mm)
94	0.34	4000	3000

TABLE IV. LAMINA PROPERTIES - SKIN

E_1 (GPa)	**E_2 (GPa)**	**G (GPa)**	**v12**	**etu1 (μmm/mm)**	**ecu1 (μmm/mm)**
133	9.3	3.7	0.34	5565	4181

Three laminate configurations are evaluated, a soft laminate with a high percentage of 45 degree fibers, a quasi-isotropic laminate and a hard laminate with a high percentage of 0 degree fibers. The effective laminate stiffness properties for each laminate configuration are listed in Table 5.

TABLE V. LAMINATE PROPERTIES - SKIN

Ply Angle Percentages (%0/%45/%90)	**E_1 (GPa)**	**E_2 (GPa)**	**G (GPa)**
10/80/10	31	29	28
25/50/25	50	47	19
60/30/10	89	83	13

SIZING RESULTS

TABLE VI. SIZING RESULTS

Anisogrid Concepts	**δ_a (mm)**	**δ_c (mm)**	**δ_h (mm)**	**a_c (mm)**	**Φ (deg)**	**h (mm)**	**Skin Layup (0/45/90)**	**Unit Weight (Kg/m^2)**
1	N/A	3	7	110	25	21	N/A	5.06
2	10	4	8	115	37.5	19	N/A	5.15
3	N/A	2.5	0.8	103	35	19	25/50/25	5.17

PANEL STIFFNESS

The panel stiffness verification is performed by constructing a verification FEM of structural concept 1. Four unique load conditions are applied obtain the load-strain and moment-curvature response. The responses are used to back-out the panel level ABD stiffness terms and verify the analytically-computed panel-level stiffnesses [2]. The stiffnesses are also verified with a published analytical method for calculating panel stiffnesses for anisogrid structure without skin [1].

TABLE VII. PANEL STIFFNESS VARIFICATION

Panel Stiffness	**Units**	**Description**	**HyperSizer**	**Analytical Method [1]**	**FEA Model**
A11	N/mm	axial stiffness	177,700	177,614	178,001
A22	N/mm	radial stiffness	87,420	87,398	87,612
A33	N/mm	shear stiffness	59,220	59,205	59,380
D11sym	$N\text{-}mm^2/mm$	Symmetric axial bending stiffness	8,527,000	8,525,489	8,605,351
D22sym	$N\text{-}mm^2/mm$	Symmetric radial bending stiffness	4,196,000	4,195,082	4,302,675
D33sym	$N\text{-}mm^2/mm$	Symmetric shear bending stiffness	2,842,000	2,841,830	2,932,592

Ainsworth J. James, Collier Research, Corp., 760 Pilot House Dr., Newport News, VA U.S.A.
Niemann Steffan, DLR, Lilienthalplatz 7 38108 Braunschweig, Germany.

LOCAL RIB STRESS DISTRIBUTION

TABLE VII. RIB STRESS VERIFICATION

Panel Object	Stress	Units	Description	HyperSizer	Analytical Method [2]	FEA Model
Load Case 1: Nx = -592 (N/mm)						
Angle Web -	σ11	N/mm^2	Stress in angle web 1	-234.92	-235.0	-234.5
Angle Web +	σ11	N/mm^2	Stress in angle web 2	-234.92	-235.0	-234.5
Circum Web	σ11	N/mm^2	Stress in circum web	274.07	274.1	273.8
Load Case 2: Nx = -592 (N/mm), Nxy = 65 (N/mm)						
Angle Web -	σ11	N/mm^2	Stress in angle web 1	-279.6	-279.7	-280
Angle Web +	σ11	N/mm^2	Stress in angle web 2	-190.24	-190.3	-190
Circum Web	σ11	N/mm^2	Stress in circum web	274.07	274.1	272
Load Case 3: Nx = -198 (N/mm), Nxy = 160 (N/mm)						
Angle Web -	σ11	N/mm^2	Stress in angle web 1	-188.5		-183
Angle Web +	σ11	N/mm^2	Stress in angle web 2	31.4		30.9
Circum Web	σ11	N/mm^2	Stress in circum web	91.6		90.8

RIB BUCKLING

Figure 3 illustrates the rib column buckling mode for the anisogrid ribs without skin. Figure 4 shows the linear relationship between cross sectional EI bending stiffness and buckling Eigenvalue.

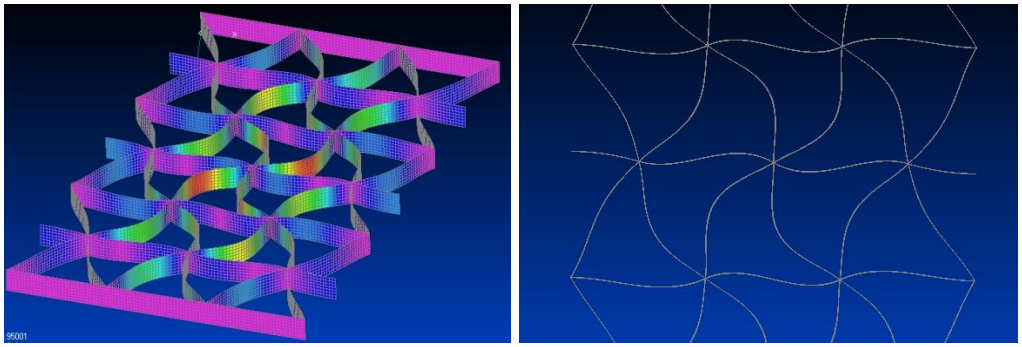

Figure 3. Anisogrid rib buckling mode shape

Ainsworth J. James, Collier Research, Corp., 760 Pilot House Dr., Newport News, VA U.S.A.
Niemann Steffan, DLR, Lilienthalplatz 7 38108 Braunschweig, Germany.

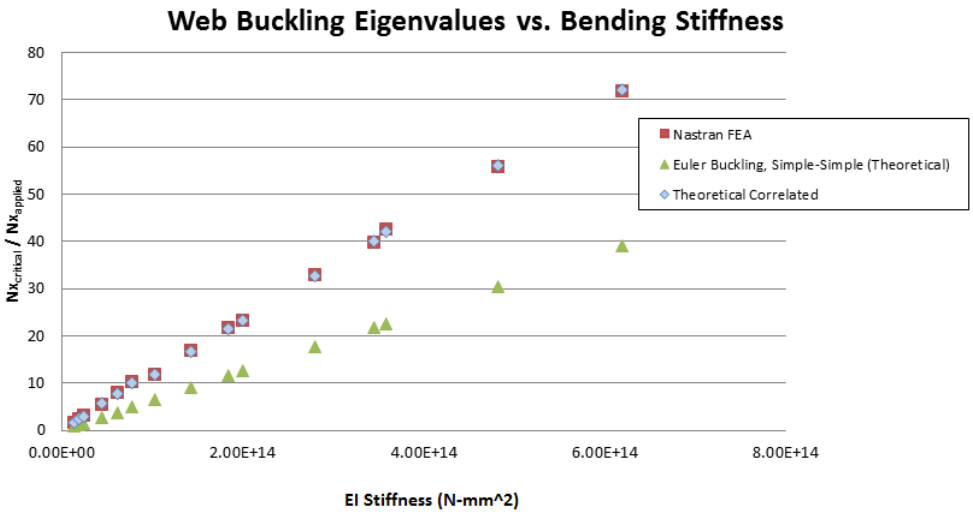

Figure 4. Sensitivity of rib buckling eigenvalues to varying rib stiffness

Figure 4 shows the FEA buckling solution is more sensitive to the increasing rib EI bending stiffness because the FEA eigenvalue captures the additional rotational fixity at the joints. This rotational fixity is not captured in the 'theoretical' Euler column bucking solution. By studying the buckling mode shapes, figure X.X, it is clear that the circumferential and angle ribs are both providing rotational rigidity to the joint. By correlating the analytical buckling predictions with FEA results, shown in figures 5 and 6, a rotational fixity buckling coefficient (K) is derived as:

$$K = \left(0.4579\left(\frac{\boldsymbol{\delta c}}{\boldsymbol{\delta h}}\right)^2 - 0.0464\left(\frac{\boldsymbol{\delta c}}{\boldsymbol{\delta h}}\right) + 0.59\right)(-0.0175(\boldsymbol{\delta c}) + 1.88) \qquad (1)$$

Where $\boldsymbol{\delta c}$ and $\boldsymbol{\delta h}$ represent the thickness of the circumferential and helical ribs respectively. By including the rotational fixity coefficient in the rib buckling analysis the 'theoretical correlated' eigenvalue prediction matches the FEA solution, as seen in figure 4.

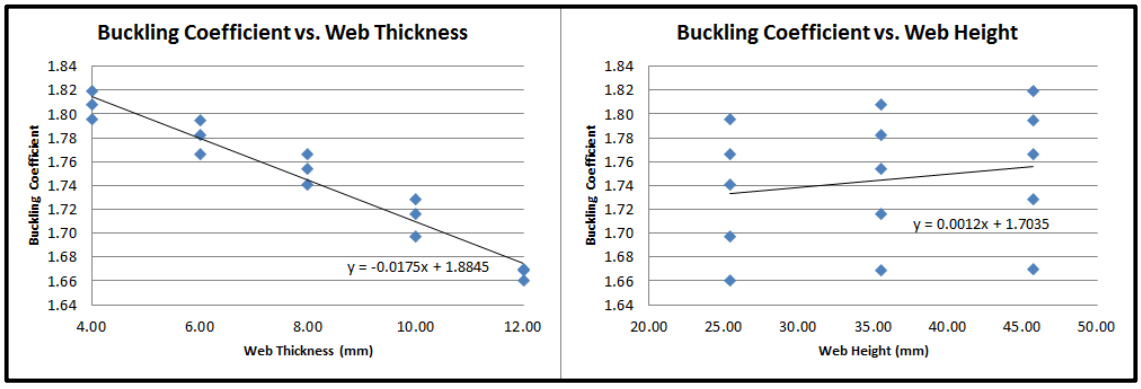

Figure 5. Sensitivity of rib buckling coefficient to varying rib thickness and height

Ainsworth J. James, Collier Research, Corp., 760 Pilot House Dr., Newport News, VA U.S.A.
Niemann Steffan, DLR, Lilienthalplatz 7 38108 Braunschweig, Germany.

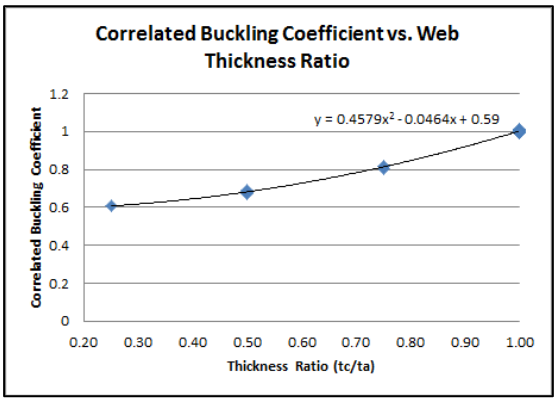

Figure 6. Sensitivity of correlated rib buckling coefficient to varying rib thickness ratio ($\boldsymbol{\delta_c/\delta_a}$)

Figure 5 shows the sensitivity of the buckling coefficient ($EV_{FEA}/Th_{eoretical}$) to varying web thickness and web height. The scatter of the three data points at each rib thickness represents the influence of varying the rib height between 25mm, 36mm and 46mm. By studying the plots it is observed that the buckling coefficient is 15 times more sensitive to changing the thickness than changing the height of the ribs. This makes physical sense because the cross sectional moment of inertia relative to the 'weak' axis of the beam (I_2), is more sensitive to changing the thickness of the ribs (δ). Using the equation for the buckling coefficient shows excellent agreement to the FEA results. However, this buckling coefficient is only valid for grid cross sections where the circumferential and helical rib thicknesses are equivalent (rib thickness ratio, $\boldsymbol{\delta_c/\delta_a}$ = 1.0). Figure 6 represents the sensitivity of the correlated buckling coefficient ($EV_{FEA}/Co_{rrelated}$) to the rib thickness ratio ($\boldsymbol{\delta_c/\delta_a}$). Table 8 represents the mass impact of including the rotational fixity coefficient in the rib buckling analysis during sizing.

TABLE VIII. MASS IMPACT OF INCLUDING FIXITY COEFFICIENT

Structural Concept	Theoretical (kg/m^2)	Correlated (kg/m^2)	Reduction (%)
1	5.54	5.06	8.6
2	5.47	5.15	5.8
3	5.17	5.17	N/A

GLOBAL BUCKLING

Rayleigh-Ritz SS8 [3] is used to compute shell buckling Eigenvalues for cylindrical barrels for each structural concept. The SS8 solution is verified against a second analytical method [2] and linear, FEA numerical Eigenvalue solutions (MSC Nastran SOL105). A comparison of the two analytical and numerical FEA solutions is provided in table 7, for structural concept 1.

TABLE IX. GLOBAL BUCKLING EIGENVALUE COMPARISON

HyperSizer (Rayleigh Ritz) [3]	Analytical Method [1]	Nastran, Solution 105
1.285	1.283	1.286

Ainsworth J. James, Collier Research, Corp., 760 Pilot House Dr., Newport News, VA U.S.A.
Niemann Steffan, DLR, Lilienthalplatz 7 38108 Braunschweig, Germany.

OBSERVATIONS

For all concepts, the controlling failure modes are panel (global) buckling, composite strength and local stability of the ribs in compression. The height of the ribs is driven by the global buckling criteria. The strain coupling is observed by studying the local stresses in the ribs. The circumferential ribs are in tension because they are being pulled by the angle ribs which are in compression. So the angle and axial ribs are strength and buckling critical and the circumferential ribs are strength critical.

For the concepts without skin, the ribs are the primary compression carrying structure. In these concepts the ribs are sized to prevent local column buckling. This buckling criteria is driving the t/H ratio to increase. Since the thickness has more contribution to the rib cross sectional EI2 (buckling axis), ribs with higher t/H ratios are more stable in column buckling.

The concept with skin has thinner ribs with a lower t/H ratio. Since the skin supports the ribs along the length, the ribs are not susceptible to column buckling. The buckling mode of these ribs is assumed is more like a plate with SSSF conditions. By studying the object loads we observe the skin and ribs are sharing the compression load. As a result, the skin is local buckling critical. For this study, the skin is required to stable up to ultimate load. There may be additional mass saving opportunity to by allowing the skin to postbuckle.

CONCLUSIONS

The unit weights of each structural concept are within 2%. The study shows there is not a significant mass savings opportunity for excluding the skin, however if there are system-level advantages to manufacturing a grid structure without skin, this study proves the concept is a viable and weight competitive option.

REFERENCES

1. Vasiliev VV, Razin AF. Anisogrid composite lattice structures - Development and aerospace applications. Compos Struct 2012;94:1117-1127.
2. Collier, C. (1993). Stiffness, Thermal Expansion, and Thermal Bending Formulation of Stiffened, Fiber-Reinforced Composite Panels. AIAA/ASME/ASCE/AHS/ASC Structures, Structural Dynamics and Materials Conference, 34th. La Jolla: AIAA-1993-1569.
3. Leissa, A. (1985). Buckling of Laminated Composite Plates And Shell Panels. AFWAL-TR-85-3069 Air Force Flight Dynamics Laboratory.

Ainsworth J. James, Collier Research, Corp., 760 Pilot House Dr., Newport News, VA U.S.A.
Niemann Steffan, DLR, Lilienthalplatz 7 38108 Braunschweig, Germany.